



PAPER • OPEN ACCESS

Evaluation of different general $V(\lambda)$ mismatch indices of photometers for LED-based light sources in general lighting applications

To cite this article: Udo Krüger *et al* 2022 *Metrologia* **59** 065003

View the [article online](#) for updates and enhancements.

You may also like

- [KEPLER Mission: development and overview](#)
William J Borucki
- [Development of white LED illuminants for colorimetry and recommendation of white LED reference spectrum for photometry](#)
Alexander Kokka, Tuomas Poikonen, Peter Blattner *et al.*
- [Robot goniophotometry at PTB](#)
M Lindemann, R Maass and G Sauter

Evaluation of different general $V(\lambda)$ mismatch indices of photometers for LED-based light sources in general lighting applications

Udo Krüger^{1,*} , Alejandro Ferrero² , Ville Mantela³ ,
Anders Thorseth⁴ , Klaus Trampert⁵ , Olivier Pellegrino⁶  and
Armin Sperling⁷ 

¹ TechnoTeam Bildverarbeitung GmbH, Ilmenau, Germany

² Instituto de Óptica, Consejo Superior de Investigaciones Científicas, Madrid, Spain

³ Metrology Research Institute, Aalto University, Finland

⁴ Technical University of Denmark, Roskilde, Denmark

⁵ Light Technology Institute, Karlsruhe Institute of Technology, Germany

⁶ Departamento de Metrologia, Instituto Português da Qualidade, Caparica, Portugal

⁷ Physikalisch-Technische Bundesanstalt, National Metrology Institute of Germany, Braunschweig, Germany

E-mail: udo.krueger@technoteam.de

Received 16 March 2022, revised 4 July 2022

Accepted for publication 5 September 2022

Published 11 November 2022



CrossMark


Abstract

The general $V(\lambda)$ mismatch index, f_1' , of a photometer quantifies the deviation between its determined relative spectral responsivity, $s_{\text{rel}}(\lambda)$, and its nominal responsivity, the spectral luminous efficiency function for photopic vision, $V(\lambda)$. LED-based light sources now dominate in general lighting, displacing incandescent and fluorescent lamps. Furthermore, the calibration of photometers will very likely see the replacement of the reference CIE standard illuminant A with CIE reference spectrum L41. The article evaluates the consequences. Should we also change the definition of the general $V(\lambda)$ mismatch index? Based on performance criteria, the individual indices are evaluated using various datasets with the help of statistical analyses. As a result, the authors can conclude that the current definition works very well even under changed calibration and application conditions and does not need to be changed. Other evaluated indices for a new index definition perform only slightly better in some cases, but do not generate generally better properties.

Keywords: spectral matching, photometer, measurement uncertainty, bootstrap, Monte Carlo, f_1'

(Some figures may appear in colour only in the online journal)

* Author to whom any correspondence should be addressed.

 Original content from this work may be used under the terms of the [Creative Commons Attribution 4.0 licence](https://creativecommons.org/licenses/by/4.0/). Any further distribution of this work must maintain attribution to the author(s) and the title of the work, journal citation and DOI.

1. Introduction

Physical measurements of photometric quantities such as luminance or illuminance are typically performed with photometers incorporating a single sensor, with a filter adapted to a spectral luminous efficiency function, or with a spectroradiometer, where the weighting is performed by subsequent calculation [1].

In general, the task of a photometer is to determine an integral photometric quantity, Y , from the spectral distribution (SD) of a light source, $S(\lambda)$, by weighted integration, according to:

$$Y = K_m \int_{360 \text{ nm}}^{830 \text{ nm}} S(\lambda)V(\lambda)d\lambda. \quad (1)$$

where $K_m \cong 683 \text{ lm W}^{-1}$, and weighting is carried out with the spectral luminous efficiency function for photopic vision, $V(\lambda)$ [1]. Other spectral luminous efficiency functions such as $V'(\lambda)$ for scotopic vision or $V_{10}(\lambda)$ for the CIE 10° photopic photometric observer can also be used, but they are not the focus of this article.

Using the spectral responsivity of the photometer, $s(\lambda)$, the luminous responsivity, s_v , is usually measured during the calibration using a calibration light source, denoted hereafter with the subscript C according to [2]:

$$s_v = \frac{\int_{\lambda_{\min}}^{\lambda_{\max}} S_C(\lambda)s(\lambda)d\lambda}{K_m \int_{360 \text{ nm}}^{830 \text{ nm}} S_C(\lambda)V(\lambda)d\lambda}, \quad (2)$$

where $S_C(\lambda)$ is the SD of the calibration light source. The handling of the integral limits is explained in appendix A.

The term ‘spectral distribution’ (‘SD’), with the symbol $S(\lambda)$, is used here in a general form for the concentration of any radiometric quantity such as irradiance or radiance as a function of wavelength [3, entry 17-21-029]. In most cases, only the relative SD is used. Currently, usually a source with a relative SD similar to the one of CIE standard illuminant A, $S_A(\lambda)$, is used for calibration [4].

Since the relative spectral responsivity of the photometer [3, entry 17-25-064], $s_{\text{rel}}(\lambda)$, can never be perfectly matched to the spectral luminous efficiency function for photopic vision, $V(\lambda)$, the luminous responsivity, s_v , of a photometer depends on the SD to be measured, and in practice it is important to evaluate the effect of the spectral $V(\lambda)$ mismatch on the measurement, and correct it, if possible.

Figure 1 shows an example for the measured relative spectral responsivity, $s_{\text{rel}}(\lambda)$, of a photometer ($s_{73}(\lambda)$, photometer #73 in the CIE S 025 dataset [5]), the $V(\lambda)$ function and the difference between both curves. The slight difference of the $s_{\text{rel}}(\lambda)$ function or mismatch to the $V(\lambda)$ function leads to errors in photometric measurements when the SD in the actual measurement is different from that used during calibration.

1.1. Quality indices

Quality indices used in photometric measurement are defined by the International Commission on Illumination (CIE) [2]. They are physical quantities with unit one, determined for specific conditions to describe specific properties of

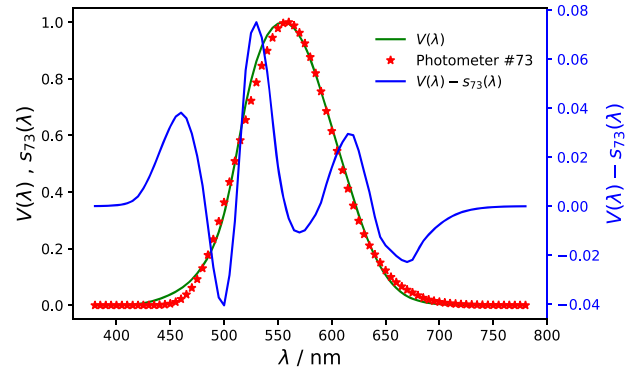


Figure 1. Measured relative spectral responsivity of the selected photometer #73, $s_{73}(\lambda)$, the target function $V(\lambda)$ and the difference between both curves.

photometers. They are positive numbers usually expressed as a percentage (symbol %). For an ideal photometer, any of the defined indices is zero, meaning the selected property is perfectly realised.

For this article, the general $V(\lambda)$ mismatch index, f'_1 , is of interest. f'_1 quantifies the mismatch between the relative spectral responsivity of a photometer, $s_{\text{rel}}(\lambda)$, and the spectral luminous efficiency function for photopic vision, $V(\lambda)$. f'_1 is used for a description of the photometric performance of photometers under general lighting conditions and for selecting photometers requiring minimal corrections under light sources with SDs different from the reference source in photometric measurements.

A perfect match between the relative spectral responsivity and $V(\lambda)$ implies that the luminous responsivity of the photometer does not depend on the relative SD of the light source to be measured. Therefore, it can be said that the general $V(\lambda)$ mismatch index indicates the sensitivity of the luminous responsivity of the photometer with respect to the variation of the relative SD of the measured light source.

f'_1 is one of the most important indices for the classification of photometers [6]. In the communication between customers and manufactures, f'_1 is often the only relevant quality index, and in several other publications, e.g. [7, 8], f'_1 is used to define selected required properties of photometers for applications to achieve a small error due to spectral mismatch.

1.2. Original f'_1 definition

Introducing the normalised spectral responsivity, $s_{\text{rel}}^*(\lambda)$

$$s_{\text{rel}}^*(\lambda) = \frac{\int_{380 \text{ nm}}^{780 \text{ nm}} S_A(\lambda)V(\lambda)d\lambda}{\int_{380 \text{ nm}}^{780 \text{ nm}} S_A(\lambda)s_{\text{rel}}(\lambda)d\lambda} s_{\text{rel}}(\lambda) \quad (3)$$

calculated using a weighting with the SD of CIE standard illuminant A, $S_A(\lambda)$ (see figure 2), f'_1 is defined as:

$$f'_1 = \frac{\int_{380 \text{ nm}}^{780 \text{ nm}} |s_{\text{rel}}^*(\lambda) - V(\lambda)|d\lambda}{\int_{380 \text{ nm}}^{780 \text{ nm}} V(\lambda)d\lambda}. \quad (4)$$

A detailed review of the historical development of f'_1 and further aspects of indices in general can be found in Krüger et al [9].

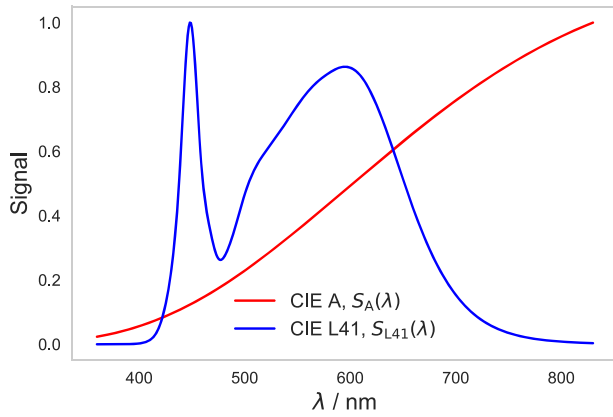


Figure 2. SD of CIE standard illuminant A, $S_A(\lambda)$, and of CIE reference spectrum L41, $S_{L41}(\lambda)$.

In previous internal studies regarding the measurement of white phosphor-based LEDs, it has been observed that calibrating a photometer according to $S_A(\lambda)$ usually results in much larger mismatch errors measuring white LED-based light sources, than calibrating according to the CIE reference spectrum L41, $S_{L41}(\lambda)$. This was reflected in a better correlation of the general $V(\lambda)$ mismatch index with the expected spectral mismatch when using CIE reference spectrum L41 for calibration and weighting.

2. Objective

Today, in the daily measurement practice of electrical lighting, almost only LED-based light sources are evaluated. Therefore, the calibration of photometers will very likely see the replacement of CIE standard illuminant A with CIE reference spectrum L41 [10]. Figure 2 shows the SDs of the two illuminants, $S_A(\lambda)$ and $S_{L41}(\lambda)$ (also referred to as $S_L(\lambda)$), respectively.

This replacement raises the question whether an update of the definition of the general $V(\lambda)$ mismatch index is necessary. A modification can be performed either by using a different normalisation than $S_A(\lambda)$ in f'_1 for the normalised spectral responsivity of the photometer, $s_{rel}^*(\lambda)$ (see equation (3)), or by introducing a different type of function for assessing this mismatch.

In this article, different versions for the general $V(\lambda)$ mismatch index are studied to assess if one of them might be more adequate when using CIE reference spectrum L41 as calibration SD. In addition, different evaluation functions are computed to rate the relationship between evaluated indices and their ability to describe the photometric performance of photometers, in terms of minimising the errors due to the spectral mismatch under general lighting conditions. The computation is carried out for all the evaluated indices based on large datasets with relative spectral responsivities of photometers and SDs of different light sources. Finally, the results will be summarised in the conclusion section.

After preliminary considerations, it was concluded that any index adequate as general $V(\lambda)$ mismatch index should have at least the following characteristics:

- To be well correlated with the expected measurement deviation from the true value when measuring an arbitrary white LED-based light source spectrally different from the calibration light source. This deviation is called hereafter ‘expected spectral mismatch deviation’.
- To be independent of a specific set of test light sources, i.e. its definition must not include a specific set of SDs.
- To be well defined with minimal requirements for the spectral bandwidth and spectral resolution.
- To be easy to implement and to be readily understood by manufacturers and users.

3. Definition of evaluated indices

Definitions of the evaluated indices studied in this work, as alternative of f'_1 , are given below. Note that they are not defined as percentages for readability.

3.1. Classic indices

Classic indices only differ from f'_1 as defined in equation (4) by a normalisation factor, α_X , of the relative spectral responsivity, which is defined as:

$$\alpha_X = \frac{s_{rel,X}(\lambda)}{s_{rel}(\lambda)} \quad (5)$$

where $s_{rel,X}(\lambda)$ is the normalised spectral responsivity of the photometer using a weighting with the SD of a general illuminant X, $S_X(\lambda)$. The following cases of a general $V(\lambda)$ mismatch index are considered:

f'_{1A} , in the case of weighting with the SD of CIE standard illuminant A, $S_A(\lambda)$, the normalisation factor is:

$$\alpha_A = \frac{\int_{380 \text{ nm}}^{780 \text{ nm}} S_A(\lambda)V(\lambda)d\lambda}{\int_{380 \text{ nm}}^{780 \text{ nm}} S_A(\lambda)s_{rel}(\lambda)d\lambda} \quad (6)$$

In this specific case, the normalised spectral responsivity is denoted as $s_{rel}^*(\lambda)$:

$$s_{rel}^*(\lambda) = \alpha_A s_{rel}(\lambda) \quad (7)$$

f'_{1E} , in the case of no SD weighting, the normalisation factor is:

$$\alpha_E = \frac{\int_{360 \text{ nm}}^{830 \text{ nm}} V(\lambda)d\lambda}{\int_{\lambda_{\min}}^{\lambda_{\max}} s_{rel}(\lambda)d\lambda} \quad (8)$$

In this case, the normalised spectral responsivity is denoted as $s_{rel,E}(\lambda)$:

$$s_{rel,E}(\lambda) = \alpha_E s_{rel}(\lambda) \quad (9)$$

f'_{1L} , in the case of weighting with the SD of CIE reference spectrum L41, $S_{L41}(\lambda)$, the normalisation factor is:

$$\alpha_L = \frac{\int_{360 \text{ nm}}^{830 \text{ nm}} S_{L41}(\lambda)V(\lambda)d\lambda}{\int_{\lambda_{\min}}^{\lambda_{\max}} S_{L41}(\lambda)s_{rel}(\lambda)d\lambda} \quad (10)$$

In this case, the normalised spectral responsivity is denoted as $s_{rel,L}(\lambda)$:

$$s_{\text{rel,L}}(\lambda) = \alpha_{\text{L}} s_{\text{rel}}(\lambda) \quad (11)$$

$f'_{1,\text{Min}}$, in this case of calculating the normalisation factor α_{Min} in a way that $\int |\alpha_{\text{Min}} s_{\text{rel}}(\lambda) - V(\lambda)| d\lambda$ is minimised with the help of an optimisation algorithm [11]:

$$\alpha_{\text{Min}} : \min_{\alpha_{\text{Min}}} \int_{360 \text{ nm}}^{830 \text{ nm}} |\alpha_{\text{Min}} s_{\text{rel}}(\lambda) - V(\lambda)| d\lambda \quad (12)$$

The normalised spectral responsivity is then denoted as $s_{\text{rel,Min}}(\lambda)$:

$$s_{\text{rel,Min}}(\lambda) = \alpha_{\text{Min}} s_{\text{rel}}(\lambda). \quad (13)$$

3.2. Fourier indices

In the following, evaluated indices based on the Fourier transform will be introduced. For this purpose, we define a difference function, $\delta_s(\lambda)$:

$$\delta_s(\lambda) = \frac{\alpha_X s_{\text{rel}}(\lambda) - V(\lambda)}{\int_{360 \text{ nm}}^{830 \text{ nm}} V(\lambda) d\lambda}. \quad (14)$$

Using this difference function and $\alpha_X = \alpha_A$ according to equation (6), the current f'_1 definition (see equation (4)) can be rewritten as:

$$f'_1 = \int_{380 \text{ nm}}^{780 \text{ nm}} |\delta_s(\lambda)| d\lambda. \quad (15)$$

For the following index definitions, the normalisation factor for the case of no SD weighting, α_E , given by equation (8) will be used. Based on the difference function and its Fourier transform, the following indices can be defined:

f''_1 , this index was introduced by Ferrero et al [12] as:

$$f''_1 = \sqrt{2 \int_0^{\nu_{\lambda,c}} |\hat{\delta}_s(\nu_{\lambda})|^2 d\nu_{\lambda}}. \quad (16)$$

In this expression, $\hat{\delta}_s(\nu_{\lambda})$ is the Fourier transform of $\delta_s(\lambda)$, ν_{λ} is the spectral frequency, and $\nu_{\lambda,c}$ is the cut-off spectral frequency. See appendix B for implementation details. However, it has to be noted that, as f''_1 and f'_1 are not quantities of the same kind, their values are not comparable directly. Since the approach of its definition is completely different, f''_1 might reveal other aspects of the difference function.

$f''_{1,\text{R}}$, this index is defined using the concept associated to f''_1 , but with a difference function, $\delta_{s,\text{R}}(\lambda)$, based on the bandwidth-limited signal that is used in equation (16).

$$\hat{\delta}_{s,\text{R}}(\nu_{\lambda}) = \begin{cases} \hat{\delta}_s(\nu_{\lambda}) & |\nu_{\lambda}| \leq \nu_{\lambda,c} \\ 0 & \text{otherwise} \end{cases} \quad (17)$$

The inverse of the Fourier transform, $\mathcal{F}^{-1} \hat{\delta}$, yields:

$$\delta_{s,\text{R}}(\lambda) = (\mathcal{F}^{-1} \hat{\delta}_{s,\text{R}}(\lambda))(\lambda) \quad (18)$$

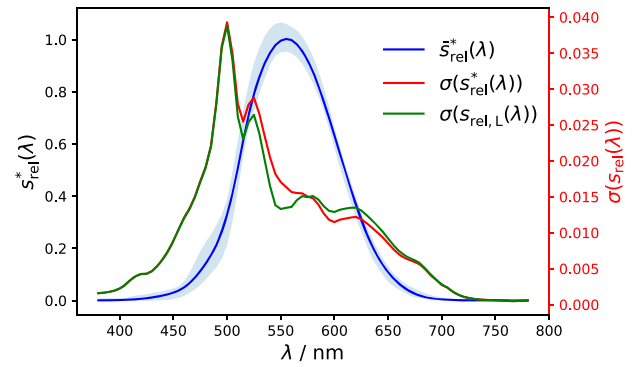


Figure 3. Mean normalised spectral responsivity $s^*_{\text{rel}}(\lambda)$ according to equation (3) (blue), the min/max band (light blue) for the CIE S 025 dataset and the standard deviation, σ , of $s^*_{\text{rel}}(\lambda)$ (red) and $s_{\text{rel,L}}(\lambda)$ (green).

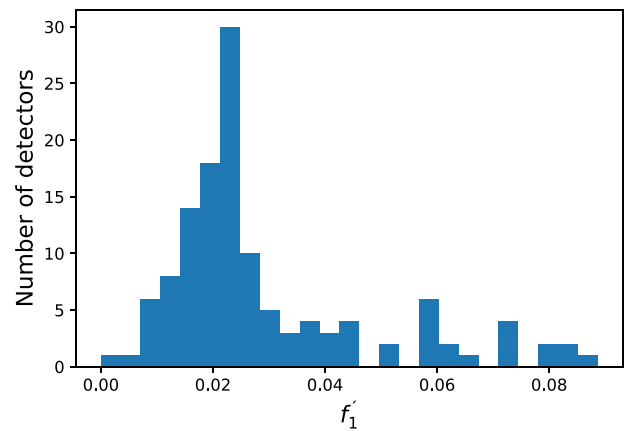


Figure 4. Histogram of the f'_1 values for the photometer CIE S 025 dataset.

With the bandwidth-limited version of $\delta_{s,\text{R}}(\lambda)$, we can calculate the index according to equation (15), leading to:

$$f''_{1,\text{R}} = \int_{\lambda_{\text{min}}}^{\lambda_{\text{max}}} |\delta_{s,\text{R}}(\lambda)| d\lambda. \quad (19)$$

The values of $f''_{1,\text{R}}$ are comparable with the usual f'_1 values and, at the same time, are fully correlated to the f''_1 values defined by equation (16).

$f'_{1,\text{BW}}$, this index makes use of bandwidth limitation for $\delta_s(\lambda)$ based on the assumption that coloured LEDs will be measured. In this case, very sharp structures in $\delta_s(\lambda)$ do not affect the measurement result. A simple symmetric model for the SD of a coloured LED, $S_{\text{LED}}(\lambda)$, (with centre wavelength λ_0 and the full-width-at-half-maximum $\Delta\lambda$), is used:

$$S_{\text{LED}}(\lambda, \lambda_0, \Delta\lambda) = \frac{1}{\Delta\lambda \sqrt{\pi / \ln(16)}} e^{-\ln(2) \cdot ((\lambda - \lambda_0) / \Delta\lambda)^2}. \quad (20)$$

The index is calculated as:

$$f'_{1,\text{BW}} = \int_{\lambda_{\text{min}}}^{\lambda_{\text{max}}} \delta_s(\lambda) * S_{\text{LED}}(\lambda, \Delta\lambda) d\lambda, \quad (21)$$

where * denotes the symbol of the convolution operation.

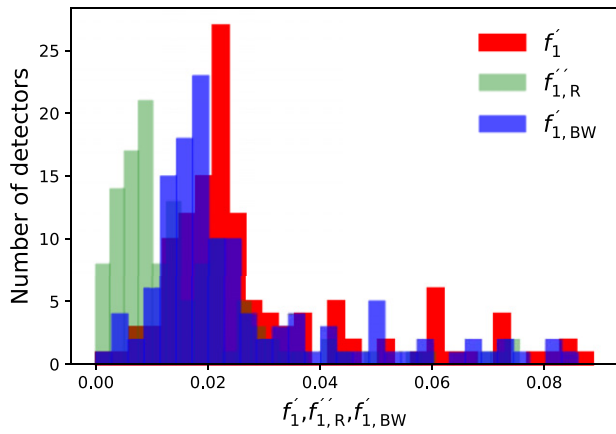


Figure 5. Histogram of the $f'_1, f''_{1,R}, f'_{1,BW}$ values for the photometer CIE S 025 dataset.

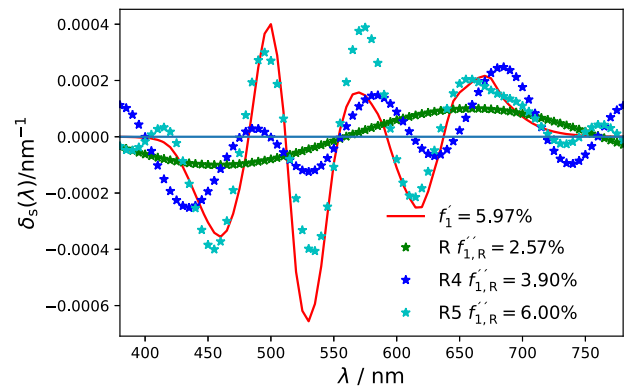


Figure 7. $\delta_s(\lambda)$ functions of photometer #73 for different cut-off frequencies R: $\nu_{\lambda,C} = 0.003 \text{ nm}^{-1}$; R4: $4 \nu_{\lambda,C}$; R5: $5 \nu_{\lambda,C}$.

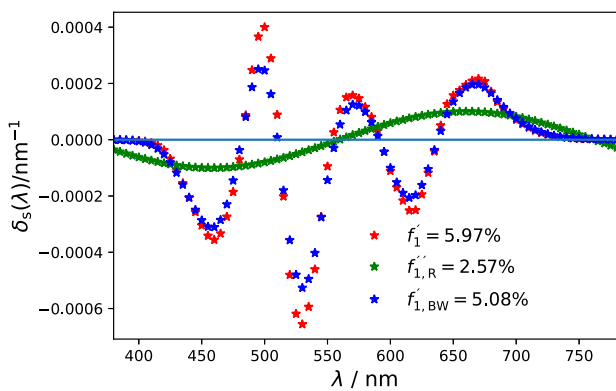


Figure 6. $\delta_s(\lambda)$ functions for different evaluated indices of photometer #73 ($\Delta\lambda = 20 \text{ nm}$; $\nu_{\lambda,C} = 0.003 \text{ nm}^{-1}$).

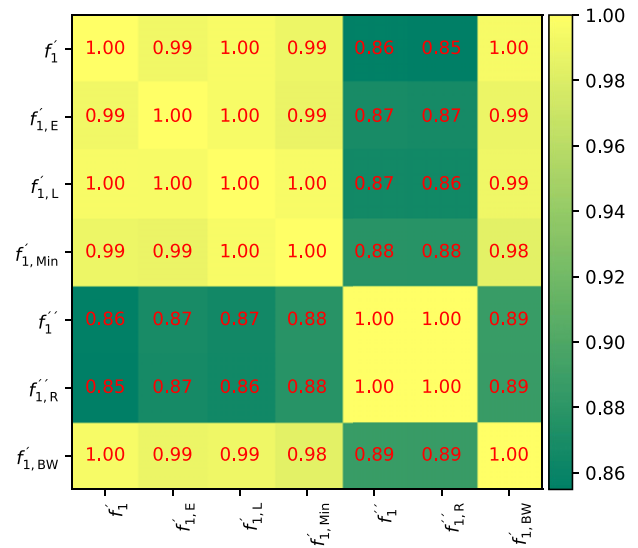


Figure 8. Correlation between the evaluated indices.

4. Comparison of the evaluated indices

This section provides some basic information about the evaluated indices and the datasets used for evaluation.

4.1. Spectral data for the evaluation

The relative spectral responsivities of 120 photometers from CIE S 025 are used for the evaluation.

For the white phosphor-based LEDs, the database from the PhotoLED project [10, 13], corresponding to 1496 SDs, is used. In addition, the database with 97 white RGB-based LEDs from CIE S 025 is used for the RGB-type calculations.

Figure 3 shows the mean normalised spectral responsivity $s_{rel}^*(\lambda)$, the min/max band for the CIE S 025 dataset and the standard deviation, σ , of $s_{rel}^*(\lambda)$ and $s_{rel,L}(\lambda)$. Figure 4 shows a histogram of the f'_1 values for the photometer CIE S 025 dataset.

4.2. Classic indices

The relative differences between the values of the classic indices and f'_1 are small, similar over the whole f'_1 interval of the dataset and usually less than 15 %. It can also be observed that the histograms of the different classic indices are very similar.

4.3. Fourier indices

In comparison with the classic indices, it can be seen that the Fourier indices generate bigger relative difference values with respect to f'_1 . For $f'_{1,BW}$, the mean relative difference lies approximately around 15 % and, for $f''_{1,R}$, around 60 % with relative differences of about 100 % in the maximum.

For the photometers used in this work, the histograms of the $f'_1, f''_{1,R}$ and $f'_{1,BW}$ values are shown in figure 5. The $f''_{1,R}$ values are significantly smaller than the f'_1 values and there is a significant compression of the range used for the photometers, whereas the $f'_{1,BW}$ values are shifted to smaller values, too, but not in the same magnitude. The $f''_{1,R}$ distribution is not shown in this figure, since its values are not directly comparable with the usual f'_1 values, but its distribution is very similar to $f''_{1,R}$ values.

Figure 6 shows the behaviour of the $\delta_s(\lambda)$ function defined in equation (14) for the different approaches.

The variation of the cut-off frequency, $\nu_{\lambda,C}$, results in significant differences of the index value. The more frequencies are used in the Fourier transform, the more equivalent is the back-transferred delta function to the original one, as shown in figure 7. In practice, the definition of a quality index should not

have parameters. Therefore, in the case of f''_1 , the parameter $\nu_{\lambda,C}$ needs to be fixed to avoid a dependency of the index value on this parameter. The cut-off frequency used here is a good choice for phosphor-type white LEDs and needs to be higher for RGB-type white LEDs.

4.4. Correlation between the evaluated indices

The linear coefficients of correlation [14] between the different values of the evaluated indices for the photometer database were calculated for comparison. Figure 8 shows that the correlation between the classic indices is very high. Only the Fourier indices f''_1 and $f''_{1,R}$ (used with the parameters above) have a lower correlation to the classic indices and could therefore have significantly different features compared to the current index.

5. Evaluation of the performances of the evaluated indices

The previously defined indices are evaluated by comparing them to the spectral mismatch correction factors (SMCF), defined in appendix A. From the datasets of photometer spectral responsivities and SDs, we need to derive different performance indicators from the SMCFs, such as standard deviations and quantiles, and estimate the coefficients of correlation, r , to the evaluated indices. We will draw conclusions about the most appropriate index by comparing the coefficients of correlation of the performance indicators to the different indices.

The SMCF values, $F_{i,j}$, are calculated using the relative spectral responsivities and the SDs in the datasets introduced in section 4. Using a specific selection from the database, we have $s_{rel,i}(\lambda), i = 0, \dots, D - 1$ relative spectral responsivities of D photometers and $S_j(\lambda), j = 0, \dots, L - 1$ SDs of L light sources.

According to the derivation in appendix A, we get the following notation for the SMCF values, $F_{i,j}$:

$$F_{i,j}(S_C(\lambda), S_j(\lambda)) = \frac{\int_{360 \text{ nm}}^{830 \text{ nm}} S_j(\lambda) V(\lambda) d\lambda}{\int_{\lambda_{\min}}^{\lambda_{\max}} S_j(\lambda) s_{rel,C,i}(\lambda) d\lambda}, \quad (22)$$

where $S_C(\lambda)$ is the SD of the calibration light source C and $s_{rel,C,i}(\lambda)$ is the relative spectral responsivity normalised with respect to that calibration source.

To make the evaluations more concise, only the absolute value of the spectral mismatch correction factor minus one, $F_{i,j}^a(S_C(\lambda), S_j(\lambda))$, will be used for further evaluation. This is probably the most significant value for a specific measurement and will be referred to hereafter as ‘absolute deviation’:

$$F_{i,j}^a(S_C(\lambda), S_j(\lambda)) = |F_{i,j}(S_C(\lambda), S_j(\lambda)) - 1|. \quad (23)$$

5.1. Evaluation based on quantiles of the SMCF

When evaluating a lot of SDs in the dataset and using the absolute deviation, a quantile-based approach can be used to get one stable number for each photometer:

$$F_{i,q+}^a = (F_{i,j}^a)_{Q=1-q} \quad (24)$$

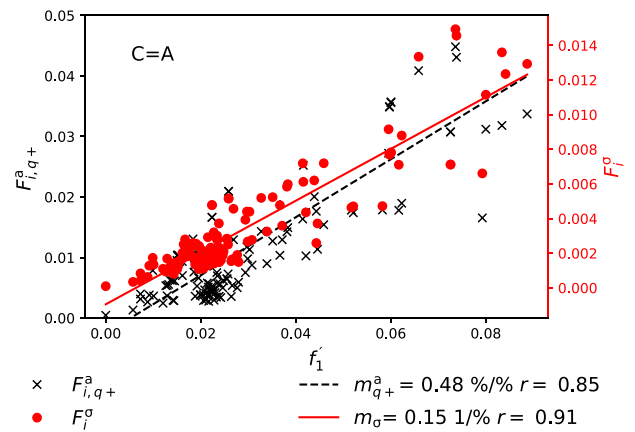


Figure 9. Absolute deviation of the spectral mismatch correction factor for phosphor-type LEDs from the PhotoLED project as light sources, and with a calibration based on CIE standard illuminant A and with respect to the current index f'_1 .

where q is the quantile (e.g. $q = 0.05$) used for evaluation and $q+$ is the short form for the upper quantile $1-q$.

To get one specific number summarising the information of all photometers, a linear regression is made

$$(m_{q+}^a, n_{q+}^a) = \text{LinReg}(f'_{1,i}, F_{i,q+}^a). \quad (25)$$

The expression $(m, n) = \text{LinReg}(x_i, y_i)$ describes a linear regression based on a least square approach for the data points (x_i, y_i) calculating the slope m and the intersection n at the origin.

The slope m_{q+}^a can be used to estimate the possible contribution of the SMCF for a specific photometer if no correction is possible because the relative spectral responsivity of the photometer or the specific SD of the light source to be measured are not known. With the f'_1 value of the photometer and the type of the SD (either of a phosphor-type LED or an RGB-type LED) one can estimate that $F^a < m_{q+}^a \cdot f'_1$ with a probability of about 95 %.

5.2. Evaluation based on the standard deviation of the SMCF

As demonstrated earlier in Mantela et al [15], the standard deviation of the spectral mismatch correction factor of each photometer over all light sources can also be used as a performance indicator:

$$F_i^\sigma(S_C(\lambda)) = \sqrt{\frac{1}{L} \sum_{j=0}^{L-1} (F_{i,j}(S_C(\lambda)) - \bar{F}_i)^2} \quad (26)$$

$$(m_\sigma, n_\sigma) = \text{LinReg}(f'_{1,i}, F_i^\sigma). \quad (27)$$

In case the photometer calibration takes place with CIE standard illuminant A, the subscript C is replaced by A. In case the photometer calibration takes place with CIE reference

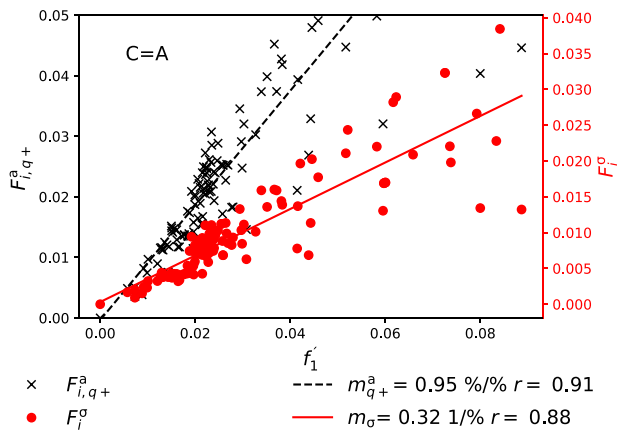


Figure 10. Absolute deviation of the spectral mismatch correction factor for RGB-based white LEDs from the CIE S 025 dataset as light sources, and with a calibration based on CIE standard illuminant A and with respect to the current index f_1' .

Table 1. Selected properties of mismatch indices for the case calibration with CIE standard illuminant A ($C = A$).

SD set	Index	$r(I, m_{q+}^a)$	$r(I, m_{\sigma})$
PhotoLED	f_1'	0.85	0.91
	$f_{1,L}'$	0.85	0.92
	$f_{1,R}''$	0.84	0.97
RGB	f_1'	0.91	0.88
	$f_{1,L}'$	0.93	0.87
	$f_{1,R}''$	0.80	0.68

Table 2. Selected properties of mismatch indices for the case calibration with CIE reference source L41 ($C = L$).

SD set	Index	$r(I, m_{q+}^a)$	$r(I, m_{\sigma})$
PhotoLED	f_1'	0.95	0.91
	$f_{1,L}'$	0.96	0.92
	$f_{1,R}''$	0.96	0.97
RGB	f_1'	0.86	0.87
	$f_{1,L}'$	0.86	0.87
	$f_{1,R}''$	0.67	0.68

spectrum L41, the subscript C is replaced by L [16]. With the database from the PhotoLED project, we get figure 9.

In figure 9, the black data points represent the upper quantile of the absolute deviation for each photometer according to equation (24) with the linear regression according to equation (25) illustrated by the black dashed line. The slope 0.48 %/ % means that we get 0.48 % SMCF for every per cent of our index value as the upper 95 % quantile.

The red points represent the standard deviation of the SMCF calculated for each photometer as defined in equation (26). The red line is the result of the linear regression with these standard deviations defined by equation (27). The slope of 0.15 1/ % means that we get a 0.15 standard deviation

of the spectral mismatch correction factor for every percent of the mismatch index.

The coefficient of correlation, r , is also indicated in the legend of the figure (figures 9 and 10).

Using RGB-type white LEDs with SDs used in CIE S025 and applying the same analysis shown before, we get results shown in figure 10.

5.3. Summary of the evaluations

From the evaluations for both calibrations with CIE standard illuminant A ($C = A$) and with CIE reference spectrum L41 ($C = L$) and all evaluated indices, we get the coefficients of correlation shown in figures 11 and 12.

Selected results can be found in tables 1 and 2.

Summarising all the data, we conclude that:

- It makes sense to focus the calculation on the determination of an upper limit using the absolute deviation and the regression line of the quantiles m_{q+}^a using equation (25); all evaluated indices make a meaningful and stable regression for phosphor-type white indicated by high r values.
- There is a significant difference in the r value for the current index definition of f_1' when changing the SD of the calibration light source from $S_C = S_A$ to $S_C = S_L$ whereas the behaviour of f_1' and $f_{1,L}'$ is very similar. The advantage of $f_{1,R}''$ is negligible for phosphor-type LEDs.
- For RGB-type white LEDs, the prediction based on $f_{1,R}''$ is no longer useful. There is a decrease of the coefficient of correlation independent from the SD of the calibration light source. This can only be changed by using a higher cut-off frequency.

5.4. Dependency on the SD and photometer dataset

Furthermore, we need to analyse whether our values (e.g. in figures 11 and 12) are stable or depend on selecting the dataset for photometers and/or light sources we use for the calculation. To this end, we introduce the bootstrap method [17], varying the photometer relative spectral responsivities and SDs used in the evaluation, implemented with a Monte Carlo simulation. The bootstrap method is used here only to estimate the standard deviation for the coefficients of correlation to verify whether valid statements can be made with respect to the calculated coefficients.

Figures 13 and 14 show that the coefficients of correlation of the evaluated indices are very stable. In this case, this means the estimation of the coefficients of correlation did not depend on the concrete selection of photometers or SDs from the dataset and are therefore reliable to evaluate the quality of the evaluated indices.

It can be seen, that the standard deviations for the coefficients of correlation using SDs of RGB LEDs are a little bit higher. But the small difference has no practical impact.

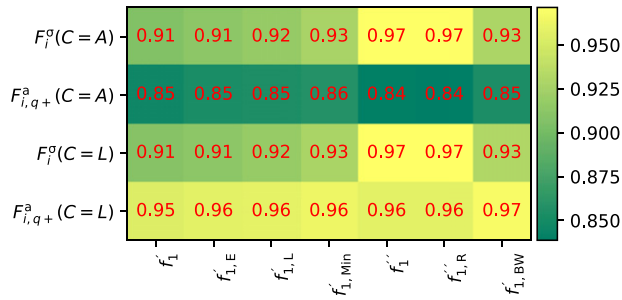


Figure 11. Coefficients of correlation for the evaluated indices with phosphor-type LEDs from the PhotoLED project as light sources.

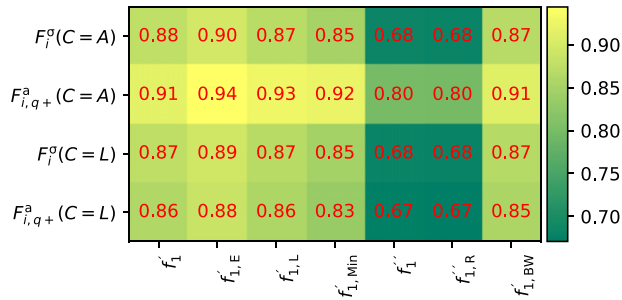


Figure 12. Coefficients of correlation for the evaluated indices with RGB-type white LEDs from CIE S 025 as light sources.

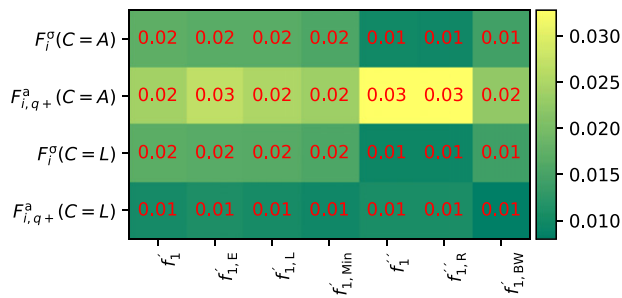


Figure 13. Standard deviation of the coefficients of correlation for the values given in figure 11 calculated using the bootstrap method.

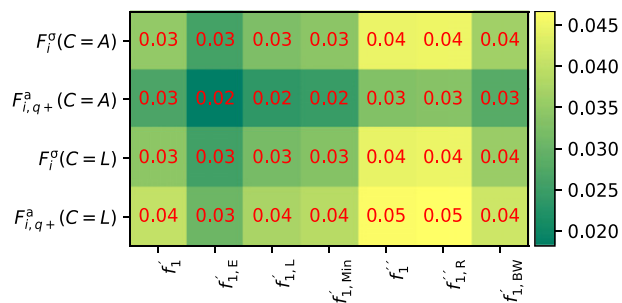


Figure 14. Standard deviation of the coefficients of correlation for the values given in figure 12 calculated using the bootstrap method.

6. Measurement uncertainty evaluation

Another important point is the determination of the measurement uncertainty for the characteristic values of the proposed indices. This is important because, during the classification of

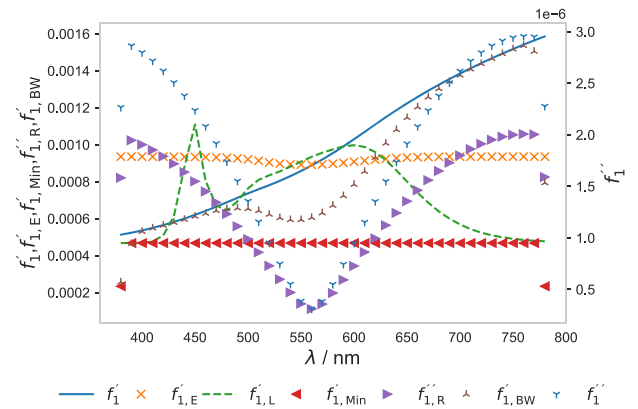


Figure 15. The influence of the normalisation for the different evaluated indices using the relative spectral responsivity of the photometer defined in equation (28).

a photometer [6], the index value and its measurement uncertainty are needed. In the case of the general $V(\lambda)$ mismatch index, the expected value of f_1' depends on the measurement uncertainty of the spectral measurements for well-matched photometers, due to the absolute value function [18, 19]. For this purpose, a Monte Carlo simulation (MC) has to be carried out in principle.

In a first step, the sensitivities are only determined for the amplitude noise and the shift of the wavelength scale separately.

6.1. Impact of the mismatch at single wavelength positions

First, we analyse the effect of the mismatch at single wavelength positions for all the evaluated indices. To do this, the index values are calculated for an ideal photometer with a small change $\Delta = 0.01$ in the relative spectral responsivity, $s_{rel}(\lambda)$, at only one wavelength position, λ_i

$$s_{rel,i}(\lambda) = \begin{cases} V(\lambda) + \Delta & \lambda = \lambda_i \\ V(\lambda) & \lambda \neq \lambda_i \end{cases} \quad (28)$$

Based on the data shown in figure 15, one can evaluate what influence a signal difference at a single wavelength position has for the different evaluated indices. The behaviour for f_1' , $f_{1,E}'$, $f_{1,L}'$ and $f_{1,Min}'$ is predictable, one can see the weighting function very clearly, but the characteristics for $f_{1,R}'$ and $f_{1,BW}'$ are somehow unexpected.

6.2. Wavelength shift

The next step is a rough estimation of the wavelength sensitivity of the quality indices. This can be analysed by shifts of $\Delta\lambda$ of the ideal photometer's relative spectral responsivity, $V(\lambda)$. In the model used inside the Monte Carlo simulation, this is represented by a correlated wavelength uncertainty contribution

$$s_{rel,\Delta\lambda}(\lambda) = V(\lambda - \Delta\lambda) \quad (29)$$

Using the data shown in figure 16, the change of the evaluated indices is about 0.02 for every nm correlated wavelength shift. This is a very critical value, which in practice means that

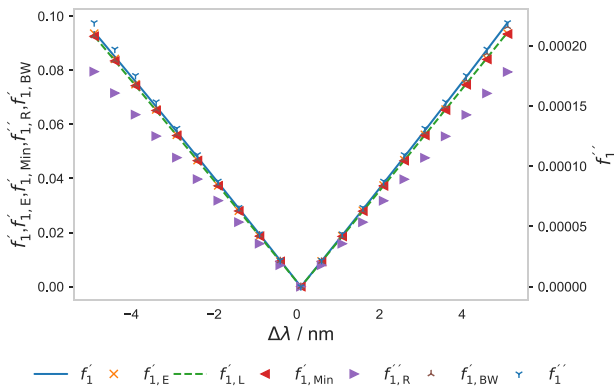


Figure 16. Change of the quality index as a function of the wavelength shift.

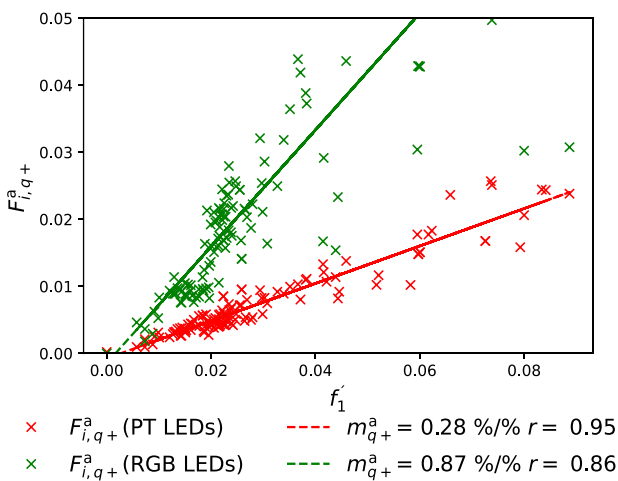


Figure 17. Upper 95 % quantiles and regression results of the SMCFs for the calibration condition $C = L$ as a function of f'_1 for phosphor-type LEDs (red, PhotoLED dataset) and RGB-type white LEDs (green, CIE S025 dataset).

great care must be taken to realise a very accurate wavelength scale when determining the relative spectral responsivities of photometers.

6.3. Measurement uncertainty contribution in photometric measurements due to the SMCF

Based on the investigations presented here, one can estimate the contribution of the SMCF in a measurement uncertainty budget for photometric measurements of white LEDs (phosphor-type and RGB-type) if only the f'_1 value of the photometer is known and no further information about the relative spectral responsivity of the photometer and the SD of the light source is available.

The presented data and regression results in figure 17 show that about 95 % of the SMCFs (absolute deviations and photometer calibration with CIE reference source L41) are smaller than $0.28 \cdot f'_1$ for phosphor-type white LEDs and smaller than $0.87 \cdot f'_1$ for RGB-type white LEDs with very high coefficients of correlation.

7. Implementation

The calculations used in this article can be found in the Python package `empir19nm02` available on GitHub [20]. There, the Python source code based on the `LuxPy` package [21] for all the specific f'_1 related calculations can be found. It contains all datasets used here for demonstration purpose. Furthermore, the package contains a Jupyter Notebook, generating all figures used in this article.

8. Discussion

This article describes and evaluates the performance of several indices for general $V(\lambda)$ mismatch under general lighting conditions based on LED light sources. They can be classified as classic indices (where the only modification with respect to the current f'_1 is the normalisation factor for the relative spectral responsivity), and those indices derived by a Fourier transform called Fourier indices.

It was found that the linear correlation between the classic indices (f'_1 , $f'_{1,E}$, $f'_{1,L}$ and $f'_{1,Min}$) is very high, which would imply that any reasonable normalisation of the relative spectral responsivity should not impact the index performance. There is also a high correlation between the two Fourier indices (f''_1 and $f''_{1,R}$). This is expected, since the latter is based on the former.

The coefficients of correlation between the different indices and statistical parameters of the absolute value of the spectral mismatch correction factor minus one (the absolute deviation), $F^a_{i,j}(S_C(\lambda), S_j(\lambda)) = |F_{i,j}(S_C(\lambda), S_j(\lambda)) - 1|$, namely the quantiles and standard deviations, have been studied using experimental data of relative spectral responsivities and SDs of white LED light sources. The aim was to classify the different indices by performance, under the assumption that the statistical parameters of $F^a_{i,j}(S_C(\lambda), S_j(\lambda))$ are related with an expected deviation from the true value due to the $V(\lambda)$ mismatch.

The initial observation that the SMCF is much better correlated to $f'_{1,L}$ than to f'_1 (see figure 18) is only due to the different calibration conditions.

When CIE reference spectrum L41 is used for the calibration, we might conclude that the Fourier indices seem to have a better performance measuring phosphor-based LEDs (broadband SDs) compared to classic indices. However, this is not the case when evaluating general lighting based on RGB LEDs (narrowband SDs). Here, classic indices have significantly better performance compared to the Fourier indices using a predefined cut-off frequency.

When the CIE standard illuminant A is used for the calibration, and general lighting based on LEDs is evaluated, both types of indices have a bad performance.

This means we can make the following more or less equal proposals for the time after changing the calibration illuminant from CIE standard illuminant A to CIE reference spectrum L41:

- Since, in practice, the value of f'_1 does not change significantly with other reasonable normalisations of the relative spectral responsivities, one option would be to keep

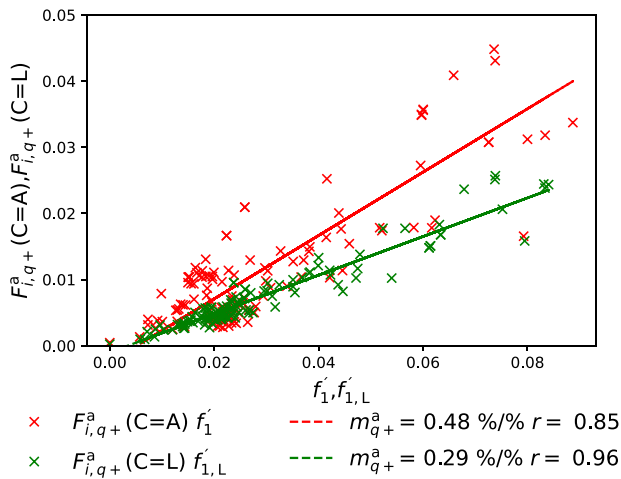


Figure 18. Upper 95 % quantiles of the SMCFs for the calibration condition $C = A$ as a function of f'_1 (red) and $C = L$ related to $f'_{1,L}$ (green).

Table 3. Summarising the index properties for selection.

Feature	Index-type	
	Classic	Fourier
Current use	+	–
Correlation with SMCF		
Phosphor-type	+	++
RGB-type	+	–
Implementation	+	o
Understanding	+	o

the current f'_1 definition without any change; this is the simplest option for customers and manufacturers;

- Change the quality index to $f'_{1,L}$; this would be in line with the original idea, which is to include the weighting with the SD of the calibration light source (which will probably be CIE reference spectrum L41 in the future) into the calculation of the normalised relative spectral responsivity, $s_{rel,X}(\lambda)$;
- An interesting option is to change the quality index to $f'_{1,E}$ or $f'_{1,Min}$; it would make the index independent of the SD of CIE standard illuminant A; this would be coherent with the idea that the spectral matching of a photometer should be independent of any form of light source SD;
- Use f''_1 as an alternative index for general lighting under phosphor-based LEDs; the advantage is that it correlates better with the $F_{i,j}^a(S_C(\lambda), S_j(\lambda))$ in those conditions; the drawback is its more complex implementation. Furthermore, one needs to change the cut-off frequency to get a good correlation to RGB-type LEDs, too.

The community is expected to decide based on the proposals and the basis laid out in this study. The following overview may be helpful using ‘+ / + +’ for pro arguments, ‘–’ for contra arguments and ‘o’ for neutral (table 3):

It should be noted that the spectral mismatch correction factor $F_{i,j}^a(S_C(\lambda), S_j(\lambda))$ allows the correction of the spectral

mismatch deviation in the specific case of measuring a specific light source with a specific SD. In contrast, the general $V(\lambda)$ mismatch index gives an indication of the mismatch but allows no correction. It is valid for describing the photometer’s expected performance when measuring an arbitrary and unknown SD of a white light source. This information can be used for a first approximation in a measurement uncertainty budget. Using a photometer calibrated with CIE reference source L41, 95 % of all SMCFs (absolute deviation) are smaller than $0.28 \cdot f'_1$ for phosphor-type white LEDs and smaller than $0.87 \cdot f'_1$ for RGB-type white LEDs with a very high coefficient of correlation.

Furthermore, the relative spectral responsivity normalised with respect to the calibration light source C , $s_{rel,C}(\lambda)$ (see equation (22)) should be provided by the manufacturer as additional information with the calibration certificates used to easily calculate the spectral mismatch correction factor in the application.

Acknowledgments

This project 19NRM02 RevStdLED has received funding from the EMPIR program co-financed by the participating states and from the European Union’s Horizon 2020 research and innovation program. Ville Mantela acknowledges partial support by the Academy of Finland Flagship Programme, Photonics Research and Innovation (PREIN), decision number: 320167. Furthermore, we thank Kevin G Smet for successfully implementing all the photometric and colorimetric functions in the LuxPy Python package, which we used to implement the calculations presented here.

Special thanks from the authors go also to the Reviewer and Peter Zwick for their valuable advice in the preparation of the article.

Appendix A. Spectral mismatch correction factor

The absolute luminous responsivity [3, entry 17-25-061], $s_{v,C}$, of a non-ideal photometer with a spectral responsivity $s(\lambda) = s_0 s_{rel}(\lambda)$ depends on the SD of the calibration light source, $S_C(\lambda)$, according to:

$$s_{v,C} = s_v(S_C(\lambda)) = \frac{s_0 \int_{\lambda_{min}}^{\lambda_{max}} S_C(\lambda) s_{rel}(\lambda) d\lambda}{K_m \int_{360 \text{ nm}}^{830 \text{ nm}} S_C(\lambda) V(\lambda) d\lambda}, \quad (30)$$

where $K_m \cong 683 \text{ lm W}^{-1}$ and s_0 is the normalisation factor for the absolute spectral responsivity $s(\lambda)$. A light source Z , with a different SD, $S_Z(\lambda)$, has a different absolute luminous responsivity, $s_{v,Z}$, accordingly:

$$s_{v,Z} = s_v(S_Z(\lambda)) = \frac{s_0 \int_{\lambda_{min}}^{\lambda_{max}} S_Z(\lambda) s_{rel}(\lambda) d\lambda}{K_m \int_{360 \text{ nm}}^{830 \text{ nm}} S_Z(\lambda) V(\lambda) d\lambda}. \quad (31)$$

Note that:

- For all integrals using $V(\lambda)$, except for the original definition of f'_1 , the lower and upper integration limits are 360 nm and 830 nm because $V(\lambda)$ is null outside this range.

- For all integrals using the photometer’s spectral responsivity, the lower and upper integration limits are λ_{\min} and λ_{\max} , the spectral limits for which the spectral responsivity of the photometer is not null. However, the integration limits to be considered should at least cover the wavelength range in which $V(\lambda)$ is defined, so that $\lambda_{\min} \leq 360$ nm and $\lambda_{\max} \geq 830$ nm.

There are two possibilities here:

- The integration limits are left at $\lambda \in [380$ nm; 780 nm] according to the current definition of f'_1 . Since especially the measurement in the interval $\lambda \in [360$ nm; 380 nm] comprises a large measurement uncertainty and the two intervals [360 nm; 380 nm] and [780 nm; 830 nm] hardly contribute to the SMCFs because $V(\lambda)$ is very small in these intervals.
- The integration limits are extended to the range 360 nm to 830 nm, since $V(\lambda)$ is defined in this interval.

The absolute luminous responsivity, $s_{v,Z}$, must be corrected using the spectral mismatch correction factor (SMCF, symbol $F(S_C(\lambda), S_Z(\lambda))$), which is the ratio of the two different luminous responsivities [2]:

$$F(S_C, S_Z) = \frac{s_{v,C}}{s_{v,Z}} = \frac{\int_{\lambda_{\min}}^{\lambda_{\max}} S_C(\lambda) s_{\text{rel}}(\lambda) d\lambda}{\int_{360 \text{ nm}}^{830 \text{ nm}} S_C(\lambda) V(\lambda) d\lambda} \cdot \frac{\int_{360 \text{ nm}}^{830 \text{ nm}} S_Z(\lambda) V(\lambda) d\lambda}{\int_{\lambda_{\min}}^{\lambda_{\max}} S_Z(\lambda) s_{\text{rel}}(\lambda) d\lambda} \quad (32)$$

Defining a more general normalisation of the relative spectral responsivity with respect to a calibration source C, $s_{\text{rel},C}(\lambda)$, using the SD of an arbitrary calibration source C, $S_C(\lambda)$, as weighting function instead of the SD of CIE standard illuminant A, $S_A(\lambda)$, and by expanding the integration limits to the spectral ranges where both, $V(\lambda)$ and $s_{\text{rel}}(\lambda)$, are not zero, one gets a modified expression of equation (3):

$$s_{\text{rel},C}(\lambda) = \frac{\int_{360 \text{ nm}}^{830 \text{ nm}} S_C(\lambda) V(\lambda) d\lambda}{\int_{\lambda_{\min}}^{\lambda_{\max}} S_C(\lambda) s_{\text{rel}}(\lambda) d\lambda} s_{\text{rel}}(\lambda) \quad (33)$$

With this definition, it is possible to rearrange the spectral mismatch correction factor as:

$$F(S_C(\lambda), S_Z(\lambda)) = \frac{\int_{360 \text{ nm}}^{830 \text{ nm}} S_Z(\lambda) V(\lambda) d\lambda}{\int_{\lambda_{\min}}^{\lambda_{\max}} S_Z(\lambda) s_{\text{rel},C}(\lambda) d\lambda} \quad (34)$$

Using equation (34) instead of equation (32) would simplify the spectral mismatch correction factor calculation if the manufacturer provides $s_{\text{rel},C}(\lambda)$ from the calibration. Furthermore, it shows the relevance of the normalisation in (33).

Appendix B. Implementation details for the Fourier indices

f''_1 : The discrete Fourier transform (DFT)⁸, of the difference function, $\delta_s(\lambda)$, defined by equation (14), is used to calculate

⁸ The DFT is an approximation of the Fourier transform. Equation (16) can be approximated with the DFT based on the sampling data that is available.

its representation in the frequency domain, $\hat{\delta}_s(\nu_\lambda)$, according to:

$$\hat{\delta}_s(\nu_\lambda) = \text{DFT}\{\delta_s(\lambda)\} \quad (35)$$

With N spectral values in the wavelength domain, $\delta_{s,i}$, the DFT results in N values in the frequency domain, $\hat{\delta}_{s,i}$. The mean value $E\{\delta_s(\lambda)\}$ and the variance $\text{Var}\{\delta_s(\lambda)\}$ with the basic rules for the DFT⁹ are obtained through:

$$E\{\delta_s(\lambda)\} = \frac{1}{N} \hat{\delta}_{s,0} \quad (36)$$

$$\text{Var}\{\delta_s(\lambda)\} = \frac{1}{N^2} \sum_{i=1}^{N-1} \hat{\delta}_{s,i}^2 \quad (37)$$

For the discrete (positive) frequencies $\nu_{\lambda,i}$, one gets $\nu_{\lambda,i} = i/(N \cdot \Delta\lambda)$ for $i = 0, \dots, N/2$. That means, for both the standard configurations where $\lambda \in [380$ nm; 780 nm] with 5 nm and 1 nm steps, the frequency step is $2.47 \times 10^{-3} \text{ nm}^{-1}$. In this article, only 5 nm steps are used for the evaluation. However, comparisons of the results of the authors showed that the differences for the f''_1 values using 1 nm or 5 nm steps are negligible.

Using a cut-off frequency $\nu_{\lambda,c}$ as parameter and the associated index $i_c = \lfloor \nu_{\lambda,c} \cdot N \cdot \Delta\lambda \rfloor$, f''_1 is calculated as:

$$f''_1 \approx \sqrt{\frac{2}{N^2} \sum_{i=1}^{i_c} \hat{\delta}_{s,i}^2} \quad (38)$$

This means that $(f''_1)^2$ is the variance of a bandwidth-limited version of $\delta_s(\lambda)$. Using the variance (without bandwidth limitation) as an index was first published by Erb [22].

ORCID iDs

Udo Krüger  <https://orcid.org/0000-0001-7729-4316>
 Alejandro Ferrero  <https://orcid.org/0000-0003-2633-3906>
 Ville Mantela  <https://orcid.org/0000-0003-0529-299X>
 Anders Thorseth  <https://orcid.org/0000-0003-4344-0770>
 Klaus Trampert  <https://orcid.org/0000-0001-6178-517X>
 Olivier Pellegrino  <https://orcid.org/0000-0003-4167-1647>
 Armin Sperling  <https://orcid.org/0000-0003-2622-243X>

References

- [1] ISO/CIE 2021 *ISO/CIE DIS 23539:2021 Photometry—the CIE System of Physical Photometry* (Vienna/Geneva: CIE—International Commission on Illumination, ISO—International Organization for Standardization)
- [2] ISO/CIE 2014 *ISO/CIE 19476:2014 Characterization and Performance of Illuminance Meters and Luminance Meters* (Vienna/Geneva: CIE—International Commission

⁹ Attention: The normalisation of the values with the number of input parameters, N , can be different for different implementations and is usually a variable option in the specific DFT implementation [23]. In the following, the full normalisation is used for the backward transform, therefore the factor $1/N$ is needed for the mean value.

- on Illumination, ISO—International Organization for Standardization)
- [3] CIE 2020 *CIE S 017/E:2020 ILV: International Lighting Vocabulary*, 2nd edn (Vienna: CIE—International Commission on Illumination) (<https://doi.org/10.25039/S017.2020>)
- [4] ISO/CIE 2022 *ISO/CIE 11664-2:2022 Colorimetry—Part 2: CIE Standard Illuminants* (Vienna/Geneva: CIE—International Commission on Illumination, ISO—International Organization for Standardization)
- [5] CIE 2015 *CIE S 025/E:2015 Test Methods for LED Lamps, LED Luminaires and LED Modules* (Vienna: CIE—International Commission on Illumination)
- [6] CIE 2019 *CIE 231:2019 CIE Classification System of Illuminance and Luminance Meters* (Vienna: CIE—International Commission on Illumination) (<https://doi.org/10.25039/TR.231.2019>)
- [7] CIE 2017 *CIE 225:2017 Optical Measurement of High-Power LEDs* (Vienna: CIE—International Commission on Illumination) (<https://doi.org/10.25039/TR.225.2017>)
- [8] CIE 2011 *CIE 194:2011 On Site Measurement of the Photometric Properties of Road and Tunnel Lighting* (Vienna: CIE—International Commission on Illumination)
- [9] Krüger U, Ferrero A, Thorseth A, Mantela V and Sperling A 2021 General $V(\lambda)$ mismatch index—history, current state, new ideas *CIE x048:2021, Proceedings of the Conference CIE 2021* (Vienna: CIE—International Commission on Illumination) pp 896–906
- [10] Kokka A et al 2018 Development of white LED illuminants for colorimetry and recommendation of white LED reference spectrum for photometry *Metrologia* **55** 526–34
- [11] Ferrero A and Thorseth A 2021 Impact of the normalization of the spectral responsivity on the performance of the general $V(\lambda)$ mismatch index *CIE x048:2021, Proceedings of the Conference CIE 2021* (Vienna: CIE—International Commission on Illumination) pp 614–49
- [12] Ferrero A, Velázquez J L, Pons A and Campos J 2018 *Index for the evaluation of the general photometric performance of photometers* *Opt. Express* **26** 18633
- [13] Jost S et al 2021 *EMPIR 15SIB07 PhotoLED - Database of LED Product Spectra* (<https://doi.org/10.11583/DTU.12783389.v2>)
- [14] Ross S M 2014 *Introduction to Probability and Statistics for Engineers and Scientist* (New York: Academic)
- [15] Mantela V, Askola J, Kärhä P and Ikonen E 2021 Novel evaluation method for general photometer mismatch index f_1' *CIE 2021—Abstr. Bookl* 174 pp –5
- [16] CIE 2018 *CIE 015:2018 Colorimetry*, 4th edn (Vienna: CIE—International Commission on Illumination) (<https://doi.org/10.25039/TR.015.2018>)
- [17] Efron B 1979 Bootstrap methods: another look at the Jackknife *Ann. Stat.* **7** 1–26
- [18] Krüger U and Sauter G 2006 Comparison of methods for indicating the measurement uncertainty of integral parameters on the basis of spectral data by means of the measurement uncertainty of the f_1' value *CIE x029:2006, Proc. 2nd CIE Expert Symp. Uncertainty, Braunschweig, Germany* (Vienna: CIE—International Commission on Illumination) p 4
- [19] Krüger U and Blattner P 2008 The influence of the uncertainty of the spectral responsivity measurement on the method of determination of f_1' *CIE x033:2008, Proc. CIE Expert Symposium in Photometry and Colorimetry, Turin, Italy* (Vienna: CIE—International Commission on Illumination) pp 49–54
- [20] Krüger Udo et al (EMPIR 19nrm02) 2022 Python Package empir19nrm02 <https://github.com/empir19nrm02/empir19nrm02> (<https://doi.org/10.5281/zenodo.7090047>)
- [21] Smet K A G 2020 Tutorial: the LuxPy Python toolbox for lighting and color science *LEUKOS* **16** 179–201
- [22] Krystek M and Erb W 1980 Kenngrößen von Empfängern *Optik* **54** 381–8
- [23] Numpy 2021 Discrete Fourier transform (numpy.fft) (<https://doi.org/10.1038/s41586-020-2649-2>)